Conduction mechanisms in amorphous carbon prepared by ion-beam sputtering

1995 J. Phys.: Condens. Matter 7 6297

(http://iopscience.iop.org/0953-8984/7/31/013)

J. Phys.: Condens. Matter 7 (1995) 6297–6315. Printed in the UK

Conduction mechanisms in amorphous carbon prepared by ion-beam sputtering

J C Dawson and C J Adkins
Cavendish Laboratory, Madingley Road, Cambridge CB3 0HE, UK

Received 20 February 1995, in final form 4 April 1995

Abstract. This paper presents novel results on the electrical properties of amorphous carbon films prepared by ion-beam sputtering. The conductivity is found to be similar to that seen in evaporated carbon. Over the range ~ 40–300 K, it is well described by the variable range hopping equation with a hopping exponent of 1/2. This indicates that the density of localized states around the Fermi energy is parabolic. An analysis of the conductivity data in terms of variable range hopping in a Coulomb gap is quantitatively consistent, indicating that this could be the origin of the parabolic shape. A second possibility is that the parabolic gap is a remnant of the graphitic density of states, which is very small at the Fermi level. Field effect measurements on the carbon films were not able to distinguish between the two models, as both could be reconciled with the observed results, although in the case of the 'graphitic' gap a large density of surface traps is required to obtain a consistent interpretation.

1. Introduction

Carbon differs from the other semiconducting group IV elements in being found in two stable bulk crystalline forms under ambient conditions, diamond and graphite, which differ greatly in their structure and properties. In diamond each of the four valence electrons is found in a hybrid sp^3 orbital, and forms a strong σ bond with an adjacent atom. Electrically it is a wide band-gap semiconductor with an energy gap of 5.5 eV, and is therefore transparent. In graphite three of the four valence electrons are in sp^2 hybrid orbitals and form σ bonds; these bonds all lie in the same plane. The fourth valence electron is found in a p_z orbital lying perpendicular to the σ bonding plane. This electron forms a weak π bond with a neighbouring p_z orbital. The resultant crystal is highly anisotropic, and is a semi-metal.

Amorphous carbon may therefore be expected to consist of a mixture of sp^3 and sp^2 bonded atoms, and to have properties intermediate between those of its crystalline counterparts. This is in fact found to be the case (Frauenheim *et al* 1989). Amorphous carbon (a-C) films can be prepared by a variety of techniques, and each produces a material with a different sp^3:sp^2 bonding ratio. This ratio and the relative arrangement of the atoms are found to be very important in determining the electronic properties of the films. A further parameter is introduced if hydrogen is added, forming hydrogenated amorphous carbon (a-C:H). In recent years attention has turned, due to its potential commercial uses, to 'diamond-like carbon' which is transparent and insulating with a high thermal conductivity. Such materials are often prepared with a high hydrogen content. The amorphous carbon films described in this paper resemble evaporated films, being non-transparent and semiconducting. Such films have been studied since the 1950s. A problem with evaporated amorphous carbon films is that they often contain large graphitic grains which were ejected bodily from the source during the deposition process (McLintock and

0953-8984/95/316297+19$19.50

Orr 1973). Preparing films by ion-beam sputtering, as here, avoids this problem since the target does not heat up enough for this process to occur.

Amorphous carbons are found to have an optical gap of 0.4–0.7 eV. Since the π states are more weakly bound than the σ states they lie closer to the Fermi level. Thus the filled π states will form the valence band and the empty π^* states the conduction band. A number of authors have attempted to predict the density of states in amorphous carbon from the atomic structure and sp^3:sp^2 bonding ratio, using various techniques. Frauenheim *et al* (1989) take a critical look at such attempts, pointing out the approximations made. Robertson and co-workers (Robertson 1986, and references therein) find that a certain amount of medium range order, i.e. clustering of the sp^2-bonded atoms into graphitic islands, is necessary in order to open up a gap at the Fermi level.

Some general features can be noted from the attempts to model the electronic and topological structure of amorphous carbon. Unlike, for example, amorphous silicon, a set of deep gap states distinct from the band edge states cannot be distinguished. Most defects are caused by breaking π bonds since this requires less energy than breaking a σ bond (which is necessary in silicon). The energy required then depends on the size of the cluster to which the defect is attached. Since the cluster size varies, a continuous density of defect states may be expected. These defect states are π-like, as are the 'band edge' states, and so the two cannot be distinguished. It is expected therefore that the density of localized states in amorphous carbon is described by the model of Cohen *et al* (1969) in which the conduction and valence band tails meet or overlap in the mobility gap.

A degree of medium range order is also found necessary to describe the properties of hydrogenated amorphous carbon (a-C:H) and diamond-like carbon (DLC) films. Both these materials contain a much larger proportion of sp^3 bonds than a-C, and this leads to a larger optical gap: $\sim$ 1.5–3 eV in a-C:H. Hydrogen stabilizes the sp^3 bonds in a-C:H, while in DLC they are able to form because of the high energies available in the deposition process. The sp^2 bonded atoms still tend to form clusters, but their extent is limited by the sp^3 bonded network. Thus the average cluster size is smaller, leading to a larger energy gap since the gap scales inversely with cluster size.

It is clear from the above discussion that the electronic properties of the various forms of carbon are intimately linked with their structures. In this paper, we report new results on the electrical properties of amorphous carbon as prepared by ion-beam sputtering, and we present a novel analysis of the data.

2. Experimental details

2.1. Sample preparation

The thin carbon films described in this paper were prepared by ion-beam sputter deposition. In this process a target is bombarded with a beam of energetic ions, causing atoms to be ejected from its surface. A film of the target material can then be formed by placing a substrate in the flux of sputtered particles. We used a graphite target, which was previously prepared by annealing in vacuum at 1300 K to release any absorbed gases. The chamber base pressure was about 5×10^{-7} mbar and a heat-sensitive label attached to the substrate holder indicated that substrate temperatures never rose above 313 K.

The ion beam is formed by extraction of (argon) ions from a plasma within an ion gun. The potential of the ions in the plasma is within a few volts of the anode potential (Harper 1983) which in this work was varied between 550–1400 V relative to ground (and therefore also to the target). Following Bellingham (1989), a further accelerating voltage of about

10% of the beam voltage was used in this work to form the beam; larger voltages tend to defocus the beam. The deposition rate achieved was about 1 nm min^{-1}. This is a fairly low rate for ion-beam sputtering, and is due to the low sputtering yield (i.e. the number of particles ejected from the target per incident ion) of carbon. Seah (1981) quotes a sputtering yield of ~ 0.4 for carbon bombarded with 500–1000 eV argon ions, which is the lowest yield of all the pure elements. The deposition parameters of all the films studied are listed in table 1.

Table 1. Deposition parameters and room temperature resistivities of the a-C films studied. V_{beam} is the ion-beam voltage; I_{beam} is the ion-beam current; r is the deposition rate; d is the thickness. Pol. Glass denotes polished soda-glass; 7059 denotes Corning 7059; Spec B denotes Spectrosil B (silica).

Film	Substrate	V_{beam}/V	I_{beam}/mA	r/nm min^{-1}	d/nm	Resistivity/Ωm
18B	7059	800	20	1.17	43	1.19×10^{-3}
19M	Glass	1000	20	1.25	39	5.55×10^{-3}
20M	Glass	650	20	0.80	39	3.84×10^{-3}
22B	Glass	800	20	1.09	9	6.10×10^{-2}
23B	Glass	800	15	0.74	43	1.08×10^{-2}
24M	Spec B	800	20	0.83	92	1.10×10^{-1}
25M	Pol. Glass	800	20	0.75	19	8.34×10^{-3}
26T	Spec B	800	20	0.48	39	2.31×10^{-2}
27T	7059	800	20	0.48	2.4	3.26×10^{-2}
28M	Spec B	800	25	0.88	39	8.83×10^{-3}
29M	Spec B	1000	30	1.35	39	2.53×10^{-3}
30M	Spec B	800	17	0.71	39	6.81×10^{-2}
31M	Spec B	1400	20	1.23	39	8.22×10^{-3}
32M	Spec B	550	13	0.34	39	3.41×10^{-2}
34T	7059	800	13	0.29	24	1.89×10^{-2}

A quartz crystal deposition monitor was positioned close to the substrate holder so that the film thickness and deposition rate could be monitored. The crystal was calibrated by measuring the thicknesses of a number of carbon films from each substrate position using a Dektak profilometer. The accuracy of the thickness measurements was only $\pm 15\%$ because of the thickness gradient along each substrate and the fact that rather thin films were used.

Various low-conductivity substrates were used for the carbon films: ordinary microscope glass, Corning 7059 and Spectrosil B for resistance measurements, and thin Spectrosil B substrates for field effect samples. Thorough cleaning was found necessary as even very small amounts of contamination (especially oil) on a substrate surface prevented the carbon films from adhering well.

The films for electrical measurements were deposited as rectangular strips 15×3.5 mm^2 with narrow side-arms for four-terminal resistance measurements. There was also a central side arm on the other side for Hall measurements. The effect of using lateral arms of finite width instead of point contacts has been analysed by Jandl *et al* (1974). In our case errors introduced are less than 0.1%. Copper wires were attached to the sample using silver paint.

Some samples were also prepared for transmission electron microscopy. These were deposited on 'holey' carbon supported on small circular gold grids. In order to ensure that a film formed across the holes, the grids were backed with collodion (cellulose nitrate). This was dissolved away after film deposition by placing the grid, collodion side down, on filter paper soaked in amyl acetate. The masks defining the geometry for the electrical measurements incorporated a hole into which these grids could be placed.

2.2. *Measurement techniques*

For electrical measurements, a constant dc current was supplied by a Keithley 602 electrometer, and the potential drop across the side-arms measured with a Keithley 604 differential electrometer amplifier. Measurements were made with the current flowing in both directions to allow for thermoelectric effects, and at two currents differing by an order of magnitude to check for any nonlinearity.

In order to measure the variation of resistance with temperature the sample was mounted on a dipstick and inserted into a CF200 continuous flow cryostat. This cryostat has a 1 T electromagnet, allowing Hall effect and magnetoresistance measurements also to be made.

Some field effect measurements were also performed on the films. For these, the films were deposited on 0.1 mm thick Spectrosil B substrates, and a gold gate electrode then evaporated on to the reverse side. The sample was mounted on a heater block held just above room temperature. The four-terminal resistance was measured as before with a variable high voltage (up to 2 kV) applied to the gate electrode. The heater block arrangement was necessary to prevent the (small) changes due to the field being swamped by resistance changes due to variation in temperature.

3. Film structure

Extensive investigations of the structure of our amorphous carbon films were not undertaken, but electron-diffraction and EELS (electron energy loss spectroscopy) measurements were made.

The electron diffraction pattern obtained from a 24 nm thick film consisted of two diffuse rings, showing that the film was amorphous. The ring diameters corresponded to distances of 0.112 and 0.207 nm. These are the same as those reported elsewhere for amorphous carbon films prepared by various methods (Devenyi *et al* 1971, Evans and Nasser 1988). The strongest diffractions in graphite are, in decreasing order of strength, 0.336 nm (002), 0.1678 nm (004), 0.1158 nm (112) and 0.203 nm (101). The latter two are close to the distances obtained from the amorphous carbon films, indicating that the bonding in these films is largely graphitic (sp^2). The first two peaks, corresponding to the (002) and (004) reflections, are missing, indicating that, as expected, there is no graphitic layering in the amorphous film.

The EELS spectrum obtained from the same film is shown in figure 1. The spectrum is again the same as that obtained from evaporated amorphous carbon (Ahn and Krivanek 1983). The large peak at 290 eV is due to excitations from 1s to $2p\sigma^*$ states, while the pre-peak at 285 eV arises from excitations to $2p\pi^*$ states (Robertson 1991) and thus indicates the presence of sp^2 bondings. The film appeared uniform; variations in the spectrum obtained from different points on the film were due to thickness variations.

A number of investigations into the structure of various forms of amorphous carbon have been published, based on a variety of diffraction and spectroscopic techniques; Robertson (1986) provides a review. Despite this, the structure of amorphous carbon is still not fully understood. The fact that film structure is strongly affected by the deposition conditions is a contributory factor. However it is generally accepted that evaporated films consist largely of sp^2 bonds, with $< 10\%$ sp^3 (Frauenheim *et al* 1989). Since the properties of our ion-beam sputtered films resemble those of evaporated carbon, it is likely that this ratio is also valid for our films, with the sp^2 bonds forming clusters up to 1.5 nm in size.

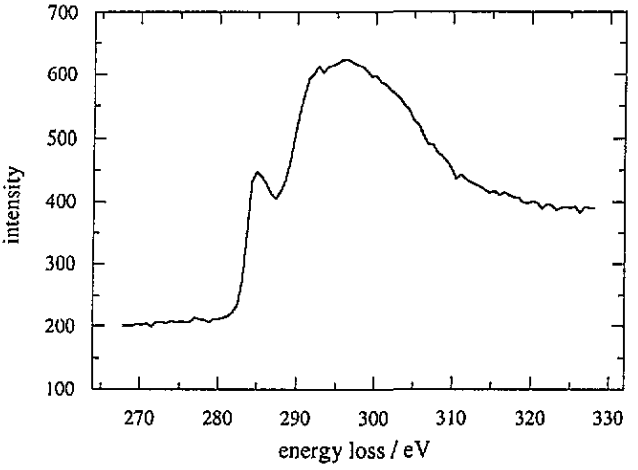

Figure 1. EELS spectrum of an amorphous carbon film.

4. Conductivity

4.1. Thickness dependence of the resistivity

Figure 2 shows the result of an experiment in which the resistivity of a film was measured as a function of thickness during the deposition process. It can be seen from this plot that the resistivity decreases sharply with increasing thickness below about 15 nm and then flattens off. This behaviour can be understood in terms of a percolation approach, as described by Shklovskii (1977) and Shklovskii and Efros (1984). In the bulk material conduction takes place along intersecting percolation paths. As the film thickness is reduced the number of such possible percolation paths is restricted, until when the film is sufficiently thin three-dimensional percolation can no longer occur. Very thin films are effectively two-dimensional. If conduction occurs by variable range hopping, this limit is reached when the film thickness d is much less than the average hop distance. Bulk three-dimensional behaviour is expected for large d.

Shklovskii and Efros (1984) show that where conduction occurs by variable range hopping, the resistivity in the intermediate regime is given by

$$\ln \rho(d) = \ln \rho(\infty) + Bd^{-1/\nu} \tag{1}$$

where B is constant at a given temperature and ν is the percolation critical exponent. In figure 3 the data of figure 2 are replotted in the form $\ln \rho$ against d^{-1}. The line is the best fit to (1) for $d > 4.5$ nm with $\ln \rho(\infty)$, B and $1/\nu$ as fitting parameters. It was not possible to obtain a good fit including lower thicknesses since (1) begins to fail as the hopping becomes two-dimensional. It can be seen that the equation describes the data well. The fitted parameters are $\rho(\infty) = (3.87 \pm 0.08) \times 10^{-2}\ \Omega$m, which is of the order of the bulk resistivities measured in the other films, and $\nu = 0.87 \pm 0.03$. This value of the critical exponent is in excellent agreement with the numerically calculated value of 0.88 (Stauffer and Aharony 1992).

4.2. Temperature-dependence of the conductivity

The conductivity of the films was measured in the range $\sim$ 40–300 K. It was not possible to extend the temperature range in either direction. The low temperature limit was set by

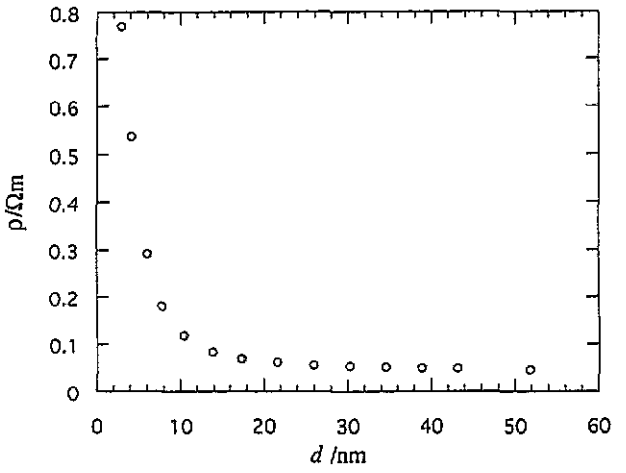

Figure 2. Thickness dependence of resistivity measured *in situ*.

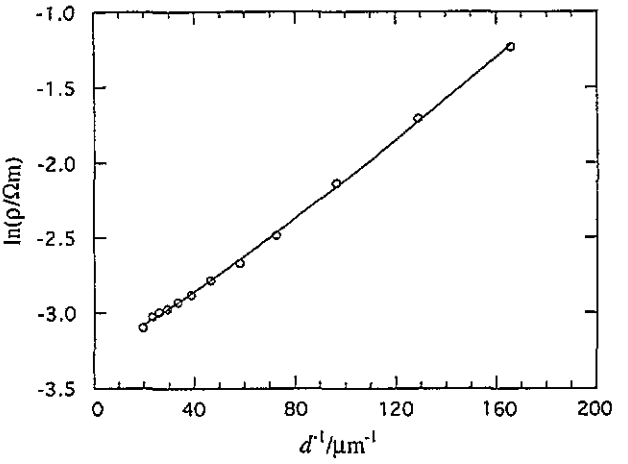

Figure 3. Thickness dependence of the resistivity, showing the fit to the model of restricted hopping paths.

the temperature at which the film resistance became unmeasurable, that at high temperature by the fact that heating the films above room temperature caused an irreversible decrease in their resistance. Such low-temperature annealing has been noted in other work (McLintock and Orr 1973), and is due to the general relaxation of disorder in the film.

The conductivity of the films listed in table 1 is plotted as a function of temperature in figure 4. All show a similar activated behaviour, the conductivity decreasing very rapidly as the temperature decreases. When the data are plotted in the form $\ln\sigma$ against T^{-1}, the results do not form straight lines but have slopes which decrease with decreasing temperature (corresponding to the activation energy decreasing), suggesting that conduction occurs by a variable range hopping process. If this is so the conductivity is expected to be of the form

$$\sigma = \sigma_0 \exp[-(T_0/T)^x] \tag{2}$$

with $x < 1$ (Mott and Davis 1979). The best values of x and T_0 for each film were obtained

by least-squares fitting to (2) using the form $\ln\sigma = \ln\sigma_0 - (T_0/T)^x$ to give equal weighting to the measurements. The results are listed in table 2. The average value of x taken over all films is 0.50 ±0.02. Also listed are values for T_0 obtained by setting $x = 0.5$ before fitting. These are denoted by T_0'.

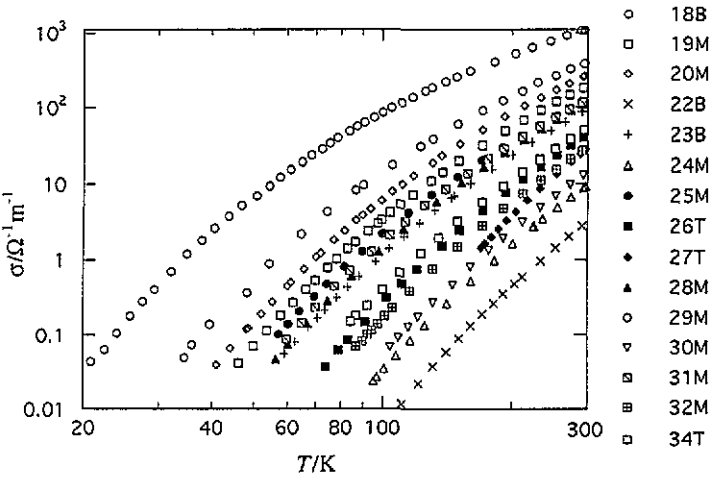

Figure 4. Variation with temperature of the conductivities of carbon films.

Table 2. Derived variable range hopping parameters. T_{min} is the lowest temperature to which measurements were made.

Film	T_{min}/K	x_{opt}	T_0/K	T_0'/K	αR_{opt}^{100}	αR_{opt}^{300}
18B	20	0.60 ± 0.02	1454 ± 6	3970 ± 30	1.58	0.91
19M	46	0.49 ± 0.01	10180 ± 20	8930 ± 20	2.36	1.36
20M	40	0.53 ± 0.02	5630 ± 10	8060 ± 20	2.24	1.30
22B	110	0.52 ± 0.03	17240 ± 40	22400 ± 60	3.74	2.16
23B	59	0.45 ± 0.02	21960 ± 50	10570 ± 40	2.57	1.48
24M	95	0.43 ± 0.01	54800 ± 100	17900 ± 100	3.34	1.93
25M	57	0.53 ± 0.01	6380 ± 20	9100 ± 20	2.38	1.38
26T	74	0.46 ± 0.04	25900 ± 100	14420 ± 70	3.00	1.73
27T	170	0.56 ± 0.05	12430 ± 50	25280 ± 90	3.97	2.29
28M	56	0.53 ± 0.02	7450 ± 40	10730 ± 20	2.59	1.50
29M	34	0.53 ± 0.03	4430 ± 40	6300 ± 60	1.98	1.15
30M	104	0.43 ± 0.02	52900 ± 200	17500 ± 200	3.31	1.91
31M	60	0.50 ± 0.03	4320 ± 30	10260 ± 40	2.53	1.46
32M	86	0.50 ± 0.01	14980 ± 70	14980 ± 70	3.06	1.77
34T	84	0.42 ± 0.03	46900 ± 200	13160 ± 90	2.87	1.66

Fits were also made to the data allowing the pre-exponential to vary with temperature, i.e. using

$$\sigma = \sigma_1 T^z \exp\left[-(T_0/T)^x\right] \tag{3}$$

with x either fixed to various values or used as a fitting parameter. This expression was not found to give a better fit to the data than that taking $z = 0$, and the extra fitting parameter

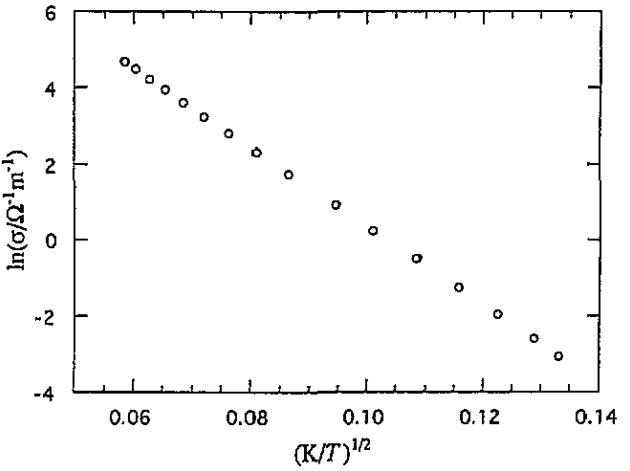

Figure 5. $\ln\sigma$ against $T^{-1/2}$ for a typical film (28M).

meant that the fits were in any case less reliable. Thus the simple hopping expression with a temperature-independent pre-exponential will be used in the following discussion.

The data for a typical film, 28M, are plotted in the form $\ln\sigma$ against $T^{-1/2}$ in figure 5. It can be seen that this provides a good straight line. The values of T_0 for all films greatly exceed T over the entire temperature range studied, as required for validity of the variable range hopping model (Adkins 1989). A further requirement is $\alpha R_{\text{opt}} > 1$, where R_{opt} is the optimum hopping length and α is the tunnelling exponent of the wavefunctions of the localized electrons. (i.e. $1/\alpha$ is the localization radius.) If this inequality is not satisfied the two hopping sites cannot be regarded as separate; their wavefunctions will hybridize. A general expression for αR_{opt} can be obtained by following Mott's optimization derivation of variable range hopping, but for a density of states $g(\varepsilon) = A|\varepsilon|^p$ where $\varepsilon = E - E_F$. This leads to

$$\alpha R_{\text{opt}} = \frac{1}{2}\left(\frac{T_0}{T}\right)^{\frac{p+1}{p+d+1}}\left(\frac{d}{p+1}\right)^{\frac{p+1}{p+d+1}}\left[\left(\frac{d}{p+1}\right)^{\frac{p+1}{p+d+1}} + \left(\frac{p+1}{d}\right)^{\frac{d}{p+d+1}}\right]^{-1} \tag{4}$$

in d dimensions which, when

$$x = \frac{p+1}{p+d+1} = \frac{1}{2} \tag{5}$$

simplifies in all dimensions to

$$\alpha R_{\text{opt}} = \frac{1}{4}\left(\frac{T_0}{T}\right)^{1/2}. \tag{6}$$

The values of this product at 100 K and 300 K are also listed for all films in table 2. (For these, the T_0' values were used.) All are greater than unity except for 18B at room temperature. This film was starting to deviate from the '$T^{1/2}$' fit near room temperature, and so the inequality is not expected necessarily to be satisfied at 300 K. The other films did not show such a deviation. Thus a-C passes the αR_{opt} test for variable range hopping.

Robertson (1988) calculated the decay length of a π defect state into other π clusters considering only nearest-neighbour interactions. A π defect is defined as any cluster with an odd number of sites and which therefore has a state at the Fermi energy. He found that the decay length is determined largely by the energy gap of the bulk cluster, which in amorphous carbon generally lies in the range 0.4–0.7 eV. Such values give a decay length ~ 1 nm. Adkins and Hamilton (1971) found a similar value (1.3 nm) from high-field measurements on evaporated amorphous carbon films. If we therefore take $\alpha^{-1} = 1$ nm, the optimum hop distance in nanometres is numerically equal to the values of αR_{opt} listed in table 2. At 100 K, $R_{opt} \sim 2.7$ nm while at 300 K $R_{opt} \sim 1.6$ nm. These values are large enough for hopping to be occurring beyond nearest neighbour sites, even if the hopping sites are in fact sp^2-bonded clusters of order 1.2 nm in diameter.

Having established that variable range hopping with a hopping exponent of 1/2 is a possible mechanism in these films, (5) can be used to obtain the form of the density of states. This depends on the effective dimensionality of the conduction process. Amorphous carbon is isotropic on the length scale relevant to hopping, and shows no evidence of any (large-scale) graphitic ordering. Therefore we take it as three-dimensional. This gives $p = 2$. This applies to all our samples, with the possible exception of 27T. The latter has an optimum hopping exponent $x = 0.6$ which places it in a transition region between two- and three-dimensional hopping, in agreement with our estimates of R_{opt}.

A parabolic density of localized states

$$g(\varepsilon) = g_2\varepsilon^2 \tag{7}$$

can arise due to the Coulomb interaction (Efros and Shkovskii 1975), or could be an intrinsic property of the material. In the latter case no further analysis of the data is possible, since we have no independent knowledge of g_2. However, the former possibility can be tested.

The Coulomb gap arises electrostatically and its shape is determined by one material parameter only, the relative permittivity of the carbon. A value for the relative permittivity of $\epsilon_r = 3.5$ was obtained from a measurement of the capacitance of a parallel-plate structure consisting of a sputtered carbon film sandwiched between two evaporated gold electrodes. The capacitance of this structure was measured at 4.2 K (to decrease the leakage current through the carbon film) and 1 kHz, with a General Radio Type 1616 precision capacitance bridge. Using the expression given by Adkins (1989), this gives for g_2 in (7), $g_2 = 3.6 \times 10^{84}\,\mathrm{J^{-3}m^{-1}} = 1.5 \times 10^{28}\,\mathrm{eV^{-3}m^{-3}}$ from which it follows that $\alpha/\mathrm{m^{-1}} = 2.9 \times 10^4 (T_0/\mathrm{K})$.

The hopping electron will only feel the Coulomb gap if its optimum hop energy W_{opt} lies within the Coulomb 'gap', i.e. within the range of energies over which the density of states continues to rise according to the Efros–Shklovskii form without reaching the background density of states, g_0. As W_{opt} increases with temperature this generally restricts the effect to low temperatures. However the conductivity of the amorphous carbon films studied here satisfies (2) with $x = 1/2$ right up to room temperature with no apparent deviation. This then sets a minimum value of the background density of states:

$$g_0/\mathrm{eV^{-1}m^{-3}} > 8.2 \times 10^{21}(\mathrm{T_0/K}) \tag{8}$$

at 300 K, since $W_{opt} = 0.5k(T_0T)^{1/2}$. The minimum g_0 thus allowed is listed for each film in table 3 as g_{0min}, along with the calculated values of α, α^{-1}, and R_{opt} at 100 K and 300 K (using the formulae given by Adkins 1989). The T_0 used are those denoted T_0' in table 2.

The localization radius (α^{-1}) is around 3–4 nm, which is not inconsistent with the thickness dependence. R_{opt} itself is also large, verifying that the electron is hopping beyond

Table 3. Coulomb-gap model parameters.

Film	$g_{0min}/eV^{-1}m^{-3}$	α/m^{-1}	α^{-1}/nm	R_{opt}^{100}/nm	R_{opt}^{300}/nm	W_{opt}/eV
18B	3.25×10^{25}	1.17×10^{8}	8.6	13.5	7.8	0.047
19M	7.31×10^{25}	2.63×10^{8}	3.8	9.0	5.2	0.071
20M	6.60×10^{25}	2.38×10^{8}	4.2	9.5	5.5	0.067
22B	1.84×10^{26}	6.62×10^{8}	1.5	5.7	3.3	0.112
23B	8.66×10^{25}	3.12×10^{8}	3.2	8.3	4.8	0.077
24M	1.47×10^{26}	5.29×10^{8}	1.9	6.3	3.7	0.100
25M	7.46×10^{25}	2.68×10^{8}	3.7	8.9	5.1	0.071
26T	1.18×10^{26}	4.24×10^{8}	2.4	7.1	4.1	0.090
27T	2.08×10^{26}	7.46×10^{8}	1.3	5.3	3.1	0.119
28M	8.78×10^{25}	3.16×10^{8}	3.2	8.2	4.7	0.077
29M	5.17×10^{25}	1.86×10^{8}	5.4	10.7	6.2	0.059
30M	1.43×10^{26}	5.15×10^{8}	1.9	6.4	3.7	0.099
31M	8.40×10^{25}	3.02×10^{8}	3.3	8.4	4.8	0.076
32M	1.23×10^{26}	4.41×10^{8}	2.3	6.9	4.0	0.091
34T	1.08×10^{26}	3.89×10^{8}	2.6	7.4	4.3	0.086

its nearest neighbours. The minimum background density of states is quite high, however. Commonly quoted values for the density of localized states in amorphous carbon are $\sim 10^{24}$–$10^{25}\,eV^{-1}m^{-3}$ (Frauenheim *et al* 1989).

The films have varying values of T_0, which depend on α and ϵ_r, and this accounts for the differences. Since the electrons are delocalized over π-bonded clusters, these parameters will depend on the number, relative arrangement and size of such clusters. These may be expected to vary between the films, leading to the variations in T_0 observed. The Coulomb gap thus provides a plausible explanation for the origin of the parabolic density of states deduced from the conductivity measurements.

5. Field effect

In these experiments, we measured changes in conductivity brought about by changing the carrier density in the films. The carrier density was varied by inducing charge electrostatically by application of an electric field normal to the sample surface. In our experiments, the electric field was applied through the substrate by varying the potential of the gate electrode deposited on the reverse side.

All samples showed the same basic field effect behaviour, the conductance decreasing with increasing positive voltage applied to the field electrode and increasing with increasing negative voltage. The maximum voltage applied to the field electrode was $\pm 2\,kV$, corresponding to a field of $\pm 2 \times 10^{7}\,Vm^{-1}$. The change in conductance was approximately linear with field. The results obtained from two films are plotted in figure 6. The fractional conductance change with the maximum potential of 2 kV applied to the field electrode never exceeded 9% and was generally around 4%. No definite correlation between the magnitude of this conductance change and the zero-field film conductivity was found.

When a positive voltage V_g is applied to the field electrode extra electrons are drawn into the film, and/or holes repelled from it; the reverse occurs when V_g is negative. Thus the effect of the applied field is to shift the Fermi level in the film. The potential V_g applied to the field electrode induces a change in the number of carriers per unit area n given by

$$\Delta n = C\Delta V_g/e \tag{9}$$

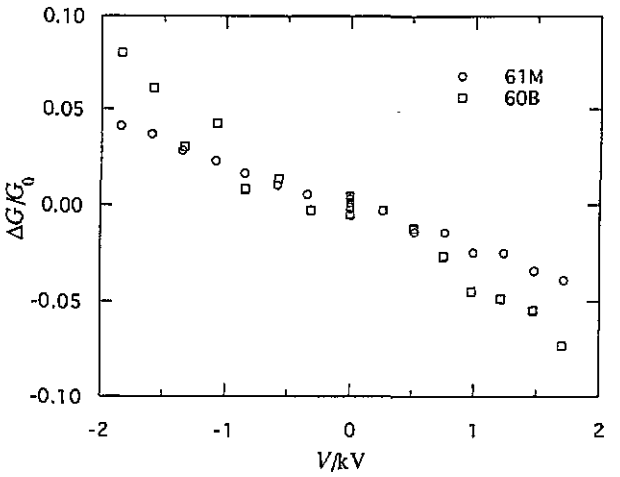

Figure 6. Typical field effect results.

where C is the capacitance per unit area between field electrode and film. If the conductivity of the film is simply proportional to the number of carriers n, as is the case when conduction occurs through extended states, then the change in conductance ΔG is simply given by

$$\Delta G = C\Delta V_g \mu w/l \tag{10}$$

where w and l are the film width and length and μ is the mobility. At first glance this theory seems appropriate to the carbon films since they show the predicted linear behaviour, the sign of the effect suggesting a conduction process dominated by holes. However the slopes of the plots give mobilities of 10^{-5}–$10^{-6}\,m^2V^{-1}s^{-1}$. These low mobilities imply that conduction is not in fact occurring via extended states, for which $\mu \sim 10^{-2}\,m^2V^{-1}s^{-1}$ is expected (Sze 1981). This supports our conclusion from the conductivity data that conduction occurs by hopping even at room temperature.

Hopping involves states close to the Fermi level. The Fermi level is shifted in a field effect experiment, and this can lead to a change in sample conductivity if the density of states, or some other relevant parameter (for example α) changes with the Fermi level. The analysis necessary in this case therefore differs from that used in other work on amorphous semiconductors, for example silicon (Madan *et al* 1976), where conduction is assumed to occur through extended states at the measurement temperature.

The size of the Fermi level shift can be obtained using Poisson's equation. If the density of states is constant and equal to g_0, the induced charge density is given by

$$\rho(x) = -e^2 g_0 \phi(x) \tag{11}$$

where $e\phi(x)$ is the shift in the Fermi energy, defined to be positive for added negative charge. A differential equation for the field E can then be obtained:

$$\frac{\partial^2 E}{\partial x^2} = -\frac{e^2 g_0}{\epsilon_0 \epsilon_r}\frac{\partial \phi}{\partial x} = \frac{e^2 g_0}{\epsilon_0 \epsilon_r} E. \tag{12}$$

As E is a function of x only, this can be solved to give

$$E(x) = E_+ e^{x/\lambda} + E_- e^{-x/\lambda}$$

where

$$\lambda = \sqrt{\epsilon_0 \epsilon_r / e^2 g_0}. \tag{13}$$

We choose $x = 0$ to be the surface of the film nearest the field electrode, i.e. at the film–substrate interface. The other surface of the film is at $x = d$, where d is the film thickness. The boundary conditions are $E(d) = 0$ and $E(0) = E_0$. The solution then becomes

$$E(x) = E_0 \frac{\sinh[(d-x)/\lambda]}{\sinh(d/\lambda)}. \tag{14}$$

Integrating this gives

$$\phi(x) = -\int E \, dx = E_0 \lambda \frac{\cosh[(d-x)/\lambda]}{\sinh(d/\lambda)} \tag{15}$$

and in particular

$$\phi(0) = \frac{E_0 \lambda}{\tanh(d/\lambda)}. \tag{16}$$

The constant of integration is zero since the Fermi energy shift at the surface is assumed to be zero when $E_0 = 0$. If there are no surface states

$$E_0 = C V_g / \epsilon_0 \epsilon_r \tag{17}$$

where ϵ_r is the relative permittivity of the dielectric. At the maximum potential used in the experiments here, $E_0 = 2.4 \times 10^7 \, \mathrm{V m^{-1}}$. Surface states can act as traps for the induced charge. If the mobility of charge in these traps is much lower than that in bulk states the observed field effect will not be as large as predicted by the arguments above.

The screening length, λ, is determined by the density of states around E_F. If $\lambda \ll d$ the Fermi level is only shifted in a small region near the $x = 0$ surface of the film. For $g_0 \sim 10^{24}$–$10^{26} \, \mathrm{eV^{-1} m^{-3}}$, $\lambda \sim 14$–$1.3 \, \mathrm{nm}$. The field effect measurements here were made on films 4–43 nm thick. If G_λ is the conductance within the screening length λ of the surface then the measured fractional change in film conductance is

$$\frac{\Delta G}{G} \approx \frac{\Delta G_\lambda}{G_\lambda} \frac{\lambda}{d}. \tag{18}$$

Thus, if $\lambda < d$, the fractional change in G should decrease as the film thickness increases, for constant induced charge. No such trend was seen. However, the large amount of scatter in the results means that it is not possible to draw any firm conclusions with regard to the magnitude of λ.

When $\lambda \gg d$ the Fermi level shift is approximately constant throughout the film. The shift necessary to accommodate the induced charge can then be obtained directly from the density of states $g(\varepsilon)$, since

$$Q/ed = \int_{E_F}^{E_F + e\phi} g(\varepsilon) \, d\varepsilon \tag{19}$$

where Q is the charge induced per unit area; $Q = C V_g$ in the absence of surface states.

The form of the temperature dependence of the conductivity suggests that the density of states around the Fermi level in these amorphous carbon films is parabolic. The interpretation of the field effect differs depending on how this parabolic dependence arises.

A Coulomb gap is tied to the Fermi level, and will therefore move if the Fermi level moves. Thus, at first sight, no field effect is expected in a system exhibiting variable range hopping in a Coulomb gap, since moving the Fermi level does not obviously change the density of states in which hopping occurs. However a change in the tunnelling exponent α will affect the conductivity, since $T_0 \propto \alpha/\epsilon_r$.

The average maximum conductance change observed in the field effect experiments was $\sim 5\%$. The actual variation in T_0 (and hence in α) necessary to provide such a change depends on the screening length, i.e. on how much of the film contributes to the effect. Since the density of states here is not constant λ cannot simply be calculated from (13). When $\lambda \gg d$ the Fermi level shift ϕ can be obtained directly from the density of states, using (19). The appropriate $g(\varepsilon)$ to use here is the background density of states. The exact form for this is not known. To obtain an estimate of ϕ, $g(\varepsilon)$ will be assumed to be a constant, N_0. Then (19) gives

$$e\phi = Q/edN_0. \tag{20}$$

A reasonable value to take for N_0 is the minimum background density of states $g_{0\min}$, which was calculated in the Coulomb gap analysis of the conductivity data. Then $N_0 \sim 1 \times 10^{26}\,\mathrm{eV^{-1}m^{-3}}$. At the maximum applied voltage of 2 kV, $Q = 8 \times 10^{-4}\,\mathrm{Cm^{-2}}$. Thus, with $d = 30\,\mathrm{nm}$, $e\phi = 0.002\,\mathrm{eV}$.

The fractional change in conductance is related to the change in T_0 by

$$\frac{\Delta G}{G} = -\frac{1}{2}\left(\frac{T_0}{T}\right)^{1/2}\frac{\Delta T_0}{T_0}. \tag{21}$$

To evaluate this an appropriate T_0 must be chosen. In the following $T_0 = 1.8 \times 10^4\,\mathrm{K}$ is taken, close to the values obtained from conductivity measurements on films with room temperature resistivities similar to those of the field effect samples. The field effect measurements were made at room temperature, so $T \sim 300\,\mathrm{K}$. A fractional conductance change of 5% then requires a 1.3% change in T_0, and hence in α. Thus if $\lambda \gg d$, a shift in the Fermi energy of 0.002 eV must lead to a fractional change in α of 1.3%. An estimate of the plausibility of this can be made as follows.

Near a band edge the energy ε of an electron in the band is related to its wavenumber k by $\varepsilon = \hbar^2k^2/2m^*$ where m^* is the effective mass. Thus a plot of ε against k^2 is a straight line. The electronic wavefunction decays into the energy gap, i.e. k is imaginary in the gap: $k = -i\alpha$. This can be plotted as in figure 7, where a smooth parabola has been drawn in the energy gap, joining the two energy band dispersion relations (m^* is taken to be the same for electrons and holes). This parabola is of the form

$$k^2 + a^2 = A\varepsilon^2. \tag{22}$$

The terms A and a^2 can be obtained from the two conditions that

$$\frac{\partial\varepsilon}{\partial k^2}(k^2 = 0) = \frac{\hbar^2}{2m^*} \tag{23}$$

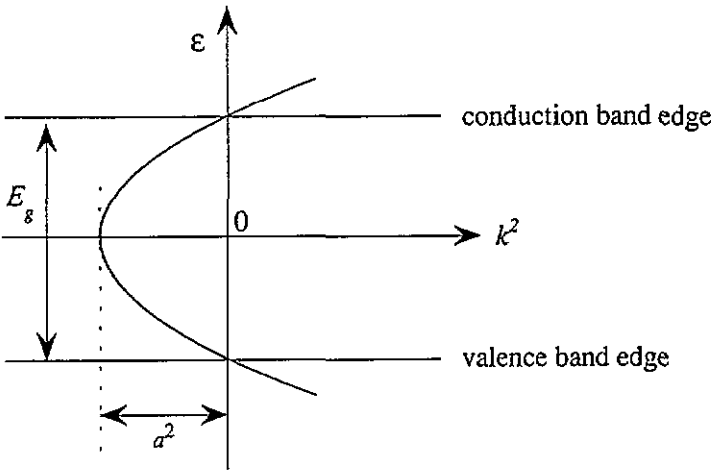

Figure 7. The energy dependence of wavenumber near the band edges.

and that $k^2 = 0$ when $\varepsilon = \pm E_g/2$, where E_g is the energy gap. Then

$$A = \frac{2m^*}{E_g\hbar^2} \tag{24}$$

$$a^2 = \frac{m^* E_g}{2\hbar^2}. \tag{25}$$

In the gap, α is given by

$$\alpha = \sqrt{a^2 - A\varepsilon^2}.$$

The effective masses in graphite are about $0.04\,m_e$ for electrons and $0.06\,m_e$ for holes (McClure 1964), where m_e is the free-electron mass. To simplify the calculation here, m^* will be taken to be the same for electrons and holes, and $m^* = 0.05\,m_e$ will be used. The energy gap in the amorphous carbon is assumed to be 0.6 eV. Then $A = 2.2 \times 10^{18}\,\mathrm{eV^{-2}m^{-2}}$ and $a^2 = 2 \times 10^{17}\,\mathrm{m^{-2}}$.

To see if these choices of m^* and E_g are reasonable, α at mid-gap ($\varepsilon = 0$) can be calculated. Using the figures above, $\alpha = 4.5 \times 10^8\,\mathrm{m^{-1}}$, which is very close to the values obtained from the analysis of the conductivity data (see table 3). Now E_F must lie below mid-gap for the field effect results to be of the form observed. Taking, for example, $E_F = -0.1$ eV, gives $\alpha(E_F) = 4.2 \times 10^8\,\mathrm{m^{-1}}$. To obtain a fractional change in α of 1.3% then requires a shift in E_F of 0.01 eV, much larger than that calculated as arising in the field effect experiment. This qualitative result is not very sensitive to the position of E_F, although the energy shift required to give any given change in α increases as E_F approaches mid-gap. Thus this interpretation cannot reconcile the field effect and Coulomb gap ideas, if $\lambda \gg d$.

When $\lambda < d$ the Fermi level shift must be calculated using (16). Choosing $\lambda = 3$ nm and $d = 30$ nm, and taking $E_0 = 2.4 \times 10^7\,\mathrm{Vm^{-1}}$, gives $\phi(0) = 0.07$ eV. With such a short screening length, less than the average hop length of ~ 4 nm, the conductance change due to the shift might be expected to be two-dimensional. However electrons can hop in and

out of the unscreened layer, and so the layer cannot be separated from the rest of the film and treated two-dimensionally. To get an estimate of the conductance change in the region affected by the field, this region is assumed to extend a distance of the order of the optimum hop length into the film. Thus the effect is largely confined to within $\sim 13\%$ of the surface of the film. A measured 5% change in conductance then requires a 10% change in T_0 and therefore in α.

Using the model described above, and again taking $E_F = -0.1\,\text{eV}$, a 10% change in α requires a shift in the Fermi level of 0.08 eV. This is very close to the shift calculated using $\lambda = 3\,\text{nm}$. If the density of states is constant such a value of the screening length corresponds to $g_0 = 2 \times 10^{25}\,\text{eV}^{-1}\text{m}^{-3}$, which is of the order of the minimum background density of states calculated from the conductivity data.

Thus the field effect results can be explained in terms of the Coulomb gap model used to interpret the conductivity. The explanation uses the fact that the tunnelling exponent (inverse localization length) decreases as a mobility edge is approached. This allows the conductivity to change even though the Coulomb gap is not altered by shifting the Fermi level. To account for the observed form of the field effect the Fermi level with no applied field must be located closer to the valence band mobility edge than to the conduction band. This is consistent with thermopower measurements on evaporated films (Devenyi *et al* 1971) which indicate that amorphous carbon is a p-type semiconductor. The size of the field effect requires that the screening length be short, much smaller than the film thickness.

If the parabolic density of states is a feature of the electronic structure of the material rather than being formed through the effect of the Coulomb interaction, then during the field effect experiment the Fermi level is moved to different points on the parabola. The interpretation of the results therefore differs from that in the previous section since the density of states in which the carriers hop changes during the experiment. An obvious difficulty in interpreting the field effect results on the basis of this model is that, while the density of states appears from the conductivity data to be symmetric, the field effect is not. If a shift in the Fermi level moves it into a higher density of states the conductivity is expected to increase. Thus an asymmetric 'parabolic' density of states, in which the two arms of the parabola increase at different rates, is not sufficient to explain the results; in this case the conductance would still increase for both positive and negative applied fields, but at different rates.

An asymmetric field effect such as that observed could be obtained if the Fermi level were displaced to one side of the parabola minimum. To obtain a decrease in conductance with positive field the Fermi level must be situated in the valence band tail, i.e. at lower energies than the parabola minimum. The size of such a displacement is limited by the fact that a variable range hopping exponent of 1/2 is observed down to at least 40 K in conductivity measurements. Thus the zero-field displacement from the parabola minimum must be less than the available thermal energy at such temperatures, i.e. $< 4\,\text{meV}$.

A first approximation to the screening length can be obtained using the density of states at the Fermi level; this is only an estimate as the density of states is not constant. Taking $T_0 = 1.8 \times 10^4\,\text{K}$, leads to

$$g(\varepsilon) = B\varepsilon^2 = 5.2 \times 10^{27}(\varepsilon/\text{eV})^2/\text{eV}^{-1}\text{m}^{-3} \tag{26}$$

where ε is measured from the parabola minimum. Thus the density of states at the Fermi energy $E_F = -0.004\,\text{eV}$ is $8.3 \times 10^{22}\,\text{eV}^{-1}\text{m}^{-3}$, and $\lambda = 50\,\text{nm}$, i.e. $\lambda > d$. The size of the shift will be greater for positive applied fields as the density of states in this direction from E_F is smaller. If the Fermi energy is displaced by δ from the parabola minimum at

zero field, then for positive applied fields

$$e\phi = \left(\frac{3Q}{Bed} - \delta^3\right)^{1/3} + \delta. \tag{27}$$

For $d = 30\,\text{nm}$ this is a shift of 50 meV.

This shift is much greater than the displacement of the zero-field Fermi level from the parabola minimum, and thus is not compatible with the field effect results, since with increasing positive field the Fermi level will move into a higher density of states once it has gone through the parabola minimum. Thus a minimum conductance would be seen in the field effect measurement, which is not the case.

The actual Fermi level shift must therefore be much smaller than that calculated above; in fact less than or of the order of $\delta = 4\,\text{meV}$. This could be achieved if there are surface states which 'soak up' the charge, reducing Q. Using the parameters chosen above, a shift of $\phi(0) = 4\,\text{meV}$ requires $Q = 5 \times 10^{-7}\,\text{Cm}^{-2}$. If N_s is the number of surface traps per unit energy and area, then

$$Q = CV - e\phi(0)N_s. \tag{28}$$

This gives $N_s \sim 1.2 \times 10^{18}\,\text{eV}^{-1}\text{m}^{-2}$. Typical surface state densities found in crystalline semiconductors are 10^{17}–$10^{18}\,\text{eV}^{-1}\text{m}^{-2}$ (Sze 1981). Thus the trap density necessary here is not impossibly high.

A smaller Fermi level shift is also obtained if λ is decreased. The value of λ required to give a shift of 4 meV at $x = 0$ can be calculated from (16). With $d = 30\,\text{nm}$ and E_0 calculated neglecting surface states, $\lambda = 0.2\,\text{nm}$ is necessary. This is too small to be reasonable. A surface state density, again $\sim 1.2 \times 10^{18}\,\text{eV}^{-1}\text{m}^{-2}$, could give a more reasonable value of $\lambda \sim 10\,\text{nm}$.

Thus this model for the density of states in amorphous carbon can be reconciled with the field effect results only if a large density of surface traps is allowed. Further experiments might allow such a distinction to be made. In particular, if higher positive fields could be applied to the field electrode it might be possible to observe the minimum in the conductance which is expected if the parabolic density of states is *not* due to a Coulomb gap. In addition, measurements of the temperature dependence of the conductivity with voltage applied to the field electrode could be informative. If conduction is occurring in a Coulomb gap a variable range hopping exponent of 1/2 should still be observed. However if the other model is appropriate, at high fields deviations may be observed from this dependence.

6. Magnetotransport measurements

Attempts were made to measure the magnetoresistance and Hall effect of the films in fields of up to 1 T. The measurements were made at room temperature as the greatly increased resistance at lower temperatures made making good measurements very difficult. In order to minimize temperature variations the measurements were performed with the sample under vacuum. An upper limit of 0.01% change over 1 T was obtained for the magnetoresistance. The upper limit to the Hall voltage of 0.4 μV corresponds to a Hall coefficient $R_H \ll 1 \times 10^{-8}\,\text{m}^3\text{C}^{-1}$, and hence the Hall mobility $\mu_H \ll 1.6 \times 10^{-5}\,\text{m}^2\text{V}^{-1}\text{s}^{-1}$. Other authors (Evans and Nasser 1988 and references therein) have also failed to measure any Hall effect in amorphous carbon films of similar resistivities to those reported here. Again this is consistent with our field effect and $\sigma(T)$ interpretations, which indicate that conduction is occurring via hopping, where the Hall mobility is expected to be very small (Mott and Davis 1979).

7. Discussion

7.1. Conductivity

A large amount of work on the properties of variously deposited amorphous carbon films has been published, and the results have been collated by Frauenheim *et al* (1989). Many of the investigations have been on evaporated and sputtered (other than ion-beam) films whose resistivities are similar to our films, and these therefore provide the best comparison for our results. In general it has been found that the temperature dependence of the conductivity can be fitted by the form

$$\sigma = \sigma_0 \exp\left[-(T_0/T)^x\right] \tag{29}$$

with $x < 1$, suggesting that conduction proceeds by variable range hopping. Shimakawa and Miyake (1988) provide the only counter-example to this dependence, as they find that the conductivity of their films prepared by rf sputtering is described by

$$\sigma \propto T^n \tag{30}$$

with $n = 15$–17. They interpret this as due to multiphonon hopping. However they note that this form does not definitely provide a better fit to their data than (29) with $x = 1/4$. Their films were also very resistive, with room-temperature resistivities of $10^6\,\Omega$m. In a later paper (Shimakawa and Kamayama 1989) they fit the same form to evaporated carbon films of resistivity $\sim 10^{-1}\,\Omega$m, finding $n = 2.6$. Equation (30) cannot be used to describe our data, as a plot of $\ln\sigma$ against $\ln T$ is not linear over any extended temperature range.

Returning to the variable range hopping (29), a number of authors have found x to lie between 1/4 and 1/2. Hauser (1977) made measurements over the range 20–300 K on getter-sputtered films with room temperature resistivities of 1–10 Ωm, and found that in films thinner than 60 nm $x = 1/3$, while in thicker films $x = 1/4$. He interpreted this as a crossover from two- to three-dimensional variable range hopping, and extracted the quantities $g(E_F) \sim 10^{24}\,\text{eV}^{-1}\text{m}^{-3}$ and $\alpha^{-1} \sim 1.2$ nm. However the optimum hop distances, obtained from the data given in his paper, are of order 10–30 nm, and therefore the 'thin' films are not in fact two-dimensional and the observed temperature dependence must have some other origin. It has been shown here that the observed increase in resistivity with decreasing film thickness can be explained by the restriction of hopping paths, without having to invoke two-dimensional behaviour.

Devenyi *et al* (1971) found that their evaporated films ($\rho \sim 3.5 \times 10^{-3}\,\Omega$m) obeyed (29) with $x = 1/4$ over the range 77–200 K, and $x = 1$ above this temperature, with an activation energy of 25 meV at 300 K. However, this is equal to the thermal energy at the measurement temperature and thus invalidates the model.

Evans and Nasser (1988) studied electron beam evaporated films with room temperatures resistivities of $2.8 \times 10^{-3}\,\Omega$m over the range 160–790 K. They found that the data could be fitted with $x = 1$ over three different temperature ranges. The activation energy below room temperature was 0.038 eV, which they interpret as due to fixed range hopping between localized defect levels. At high temperatures ($T > 625$ K) the activation energy increased to 0.458 eV, corresponding to conduction in extended states. The number of data points per fit is small. It is therefore likely, particularly at low temperatures, that the $x = 1$ fits are in fact tangents to the smooth curve actually describing the data.

Morgan (1971) fitted his results on evaporated films to (29) with $x = 1/4$, while noting that $x = 1/2$ provided a better fit. This behaviour was also observed by McLintock and

Orr (1973) and Hamilton (1972); the latter found that the appropriate value of x varied with the temperature range over which the fit was performed. Vogel *et al* (1993) assumed their ion-beam sputtered films with resistivities of 10^{-2}–$10^{-4}\,\Omega$m to be exhibiting extended state conduction; however when they fitted their data to this form they found that the fit became worse at low temperatures, and ascribed this to the fact that the band edges are not sharp (as they had assumed). However, as the fit does not appear particularly good over any part of the range (200–400 K) this conclusion seems unfounded. The activation energy of 36 meV which they obtain from their analysis is also rather small in comparison with the measured optical gap of > 0.5 eV.

From this short review of other work, it can be seen that no agreed identification of the conduction mechanism in amorphous carbon has as yet been made. In general, however, the material behaves as an amorphous semiconductor, with variable range hopping appearing to be the dominant process below room temperature and band conduction only occurring, if it does at all, at highly elevated temperatures. Our results are in agreement with this interpretation. However we are the first to describe the mechanism using the Coulomb gap, which idea was developed after much of the earlier work was done; indeed Efros and Shkovskii (1975) reviewed some of the earlier work on amorphous carbon and suggested that it could be explained qualitatively in terms of variable range hopping in a Coulomb gap. We have shown that this interpretation is also quantitatively consistent.

7.2. Field effect

Only two other reports of field effect measurements in amorphous carbon have been made. The first (Hanawa 1963) concerns arc-evaporated carbon films with room temperature resistivities of $\sim 10^2\,\Omega$m. They quote a field effect mobility of $\sim 3 \times 10^{-7}\,m^2V^{-1}s^{-1}$, and note that the sign of the field effect indicates that the majority carriers are holes. Their results are therefore similar to ours, the low mobility suggesting that hopping conduction is occurring.

The other published field effect data (Adkins *et al* 1971) were also obtained from evaporated films, with measurements being made at 77 K. It was found that conductance changes could only be measured in films less than 15 nm thick, and that the effect decreased with increasing temperature. The conductance change was roughly symmetric, with conductance increasing approximately linearly with both positive and negative fields. The conductance minimum was, however, often shifted from zero bias. This was interpreted, in conjunction with conductivity data showing a variable range hopping exponent of 1/2, as due to variable range hopping in a (fixed) parabolic density of states with the Fermi level being located a few meV from the parabola minimum. Our results differ from these, as the conductance shows no minimum. This may be due to the differing structures of the films; their evaporated films contained 'boulders' of graphite (cf McLintock and Orr 1973). It is also possible that the Adkins *et al* (1971) results relate to electrostatic relaxation effects, possibly in their glass substrates, similar to those found by Adkins *et al* (1984) in field effect experiments on discontinuous metal films.

7.3. Summary

We have found the electrical properties of amorphous carbon films prepared by ion-beam sputtering to be similar to those of evaporated carbons. The conductivity over the range $\sim$ 40–300 K is well described by the variable range hopping equation with a hopping exponent of 1/2 indicating that the density of localized states around the Fermi energy is parabolic. An analysis of the data in terms of variable range hopping in a Coulomb gap is

quantitatively consistent, indicating that this could be the origin of the parabolic shape. A second possibility is that the parabolic gap is a remnant of the graphitic density of states, which is very small at the Fermi level. Field effect measurements could not be used to distinguish between the two models, as both could be reconciled with the observed results, although in the case of the 'graphitic' gap a large density of surface traps is required to obtain a consistent interpretation.

Acknowledgments

We should like to thank the Master and Fellows of Churchill College, Cambridge, for a Research Studentship that supported one of us (JCD) during the course of this work.

References

Adkins C J 1989 *J. Physique* C **1** 1253
Adkins C J, Benjamin J D,Thomas J M D, Gardner J W and McGeown A J 1984 *J. Phys. C: Solid State Physics* **17** 1643
Adkins C J and Hamilton E M 1971 *Proc. 2nd Int. Conf. on Conduction in Low-Mobility Materials* ed N Klein, D S Tannhauser and M Pollak (London: Taylor and Francis) p 229
Ahn C C and Krivanek O L 1983 *EELS Atlas* (New York: Gatan)
Bellingham J R 1989 *PhD thesis* Cambridge University
Cohen M H, Fritzsche H and Ovshinsky S R 1969 *Phys. Rev. Lett.* **227** 1065
Devenyi A, Gheorghiu A, Belu A and Korany G 1971 *Proc. 2nd Int. Conf. on Conduction in Low-Mobility Materials* ed N Klein, D S Tannhauser and M Pollak (London: Taylor and Francis) p 215
Efros A L and Shklovskii B I 1975 *J. Physique* C **8** L49
Evans B L and Nasser G Y 1988 *Phys. Status Solidi* A **110** 165
Frauenheim T, Stephanu U, Beuriloga K, Jungnickel F, Blaudeck P and Fromm E 1989 *Thin Solid Films* **182** 63
Hamilton E M 1972 *PhD thesis* Cambridge University
Hanawa T and Kakinoki J 1964 *Carbon* **1** 403
Harper J M E, Cuomo J J and Kaufman H R 1983 *Ann. Rev. Mater. Sci.* **13** 413
Hauser J J 1977 *J. Non-Cryst. Solids* **23** 21
Jandl S, Usadel K D and Fischer G 1974 *Rev. Sci. Instrum.* **45** 1479
Kaufman H R 1986 *J. Vac. Sci. Technol.* A **3** 605
McLintock I S and Orr J C 1973 *Chem. Phys. Carbon* **11** 243
McClure J W 1964 *IBM J. Research and Development* **8** 255
Madan A, Le Comber P G and Spear W E 1976 *J. Non-Cryst. Solids* **20** 239
Morgan M 1971 *Thin Solid Films* **7** 313
Mott N F and Davis E A 1979 *Electronic Processes in Non-crystalline Materials* 2nd edn (Oxford: Oxford University Press)
Robertson J 1986 *Adv. Phys.* **35** 317
—— 1988 *Phil. Mag. Lett.* **57** 143
—— 1991 *J. Non-Cryst. Solids* **137 & 138** 825
Seah M P 1981 *Thin Solid Films* **81** 279
Shimakawa K and Kamayama T 1989 *J. Non-Cryst. Solids* **114** 786
Shimakawa K and Miyake K 1988 *Phys. Rev. Lett.* **61** 994
Shklovskii B I 1977 *Phys. Status Solidi* B **83** K11
Shklovskii B I and Efros A L 1984 *Electronic Properties of Doped Semiconductors* (Berlin: Springer)
Stauffer D and Aharony A 1992 *Introduction to Percolation Theory* 2nd edn (London: Taylor and Francis)
Sze S M 1981 *Physics of Semiconductor Devices* 2nd edn (New York: Wiley)
Vogel M, Stenzel O, Petrich R, Schaarschmidt G and Scharff W 1993 *Thin Solid Films* **227** 74